

Selective chemical vapor sensing with few-layer MoS₂ thin-film transistors: Comparison with graphene devices

R. Samnakay, C. Jiang, S. L. Rumyantsev, M. S. Shur, and A. A. Balandin

Citation: [Applied Physics Letters](#) **106**, 023115 (2015); doi: 10.1063/1.4905694

View online: <http://dx.doi.org/10.1063/1.4905694>

View Table of Contents: <http://scitation.aip.org/content/aip/journal/apl/106/2?ver=pdfcov>

Published by the [AIP Publishing](#)

Articles you may be interested in

[Growth-substrate induced performance degradation in chemically synthesized monolayer MoS₂ field effect transistors](#)

Appl. Phys. Lett. **104**, 203506 (2014); 10.1063/1.4873680

[Improving chemical vapor deposition graphene conductivity using molybdenum trioxide: An in-situ field effect transistor study](#)

Appl. Phys. Lett. **103**, 263117 (2013); 10.1063/1.4860418

[Electrical performance of monolayer MoS₂ field-effect transistors prepared by chemical vapor deposition](#)

Appl. Phys. Lett. **102**, 193107 (2013); 10.1063/1.4804546

[Detection of organic vapors by graphene films functionalized with metallic nanoparticles](#)

J. Appl. Phys. **112**, 114326 (2012); 10.1063/1.4768724

[Oxygen sensing properties at high temperatures of \$\beta\$ -Ga₂O₃ thin films deposited by the chemical solution deposition method](#)

J. Appl. Phys. **102**, 023709 (2007); 10.1063/1.2756085

An advertisement for KeySight B2980A Series Picoammeters/Electrometers. The ad features a red and white color scheme. On the left, text reads 'Confidently measure down to 0.01 fA and up to 10 PΩ' and 'KeySight B2980A Series Picoammeters/Electrometers'. Below this is a red button with the text 'View video demo'. On the right, there is an image of the device and the KeySight Technologies logo.

Selective chemical vapor sensing with few-layer MoS₂ thin-film transistors: Comparison with graphene devices

R. Samnakay,^{1,2} C. Jiang,² S. L. Romyantsev,^{3,4} M. S. Shur,³ and A. A. Balandin^{1,2,a)}

¹Phonon Optimized Engineered Materials (POEM) Center, Materials Science and Engineering Program, University of California–Riverside, Riverside, California 92521, USA

²Nano-Device Laboratory, Department of Electrical Engineering, Bourns College of Engineering, University of California–Riverside, Riverside, California 92521, USA

³Department of Electrical, Computer, and Systems Engineering, Center for Integrated Electronics, Rensselaer Polytechnic Institute, Troy, New York 12180, USA

⁴Ioffe Physical-Technical Institute, St. Petersburg 194021, Russia

(Received 19 November 2014; accepted 28 December 2014; published online 13 January 2015)

We demonstrated selective gas sensing with MoS₂ thin-film transistors using the change in the channel conductance, characteristic transient time, and low-frequency current fluctuations as the sensing parameters. The back-gated MoS₂ thin-film field-effect transistors were fabricated on Si/SiO₂ substrates and intentionally aged for a month to verify reliability and achieve better current stability. The same devices with the channel covered by 10 nm of Al₂O₃ were used as reference samples. The exposure to ethanol, acetonitrile, toluene, chloroform, and methanol vapors results in drastic changes in the source-drain current. The current can increase or decrease by more than two-orders of magnitude depending on the polarity of the analyte. The reference devices with coated channel did not show any response. It was established that transient time of the current change and the normalized spectral density of the low-frequency current fluctuations can be used as additional sensing parameters for selective gas detection with thin-film MoS₂ transistors. © 2015 AIP Publishing LLC. [<http://dx.doi.org/10.1063/1.4905694>]

Two-dimensional (2D) layered materials have attracted significant attention owing to their unusual electronic and optical properties.^{1–4} Among these material systems, semiconducting MoS₂ is one of the most promising.^{5,6} Each layer of MoS₂ consists of one sub-layer of molybdenum sandwiched between two other sub-layers of sulfur in a trigonal prismatic arrangement.⁷ A direct band gap of a single-layer MoS₂ is ~1.9 eV.^{8,9} Single-layer and few-layer MoS₂ devices have been proposed for electronic, optoelectronic, and energy applications.^{1–4,10} Recently, MoS₂ film-based field-effect transistors (FETs) were tested for sensing NO and NO₂, other gases, and water vapor.^{11–16} The sensing signal utilized in these experiments was the relative change in the resistance, $\Delta R/R$. The devices with 2D channels are natural candidates for sensor applications due to the ultimately high surface-to-volume ratio and widely tunable Fermi-level position.

In this letter, we report on selective detection of ethanol, acetonitrile, toluene, chloroform, and methanol vapors with the MoS₂ thin-film FETs (TF-FETs). The tests were conducted with the as fabricated devices and intentionally aged devices. The focus of the study was on the aged MoS₂ TF-FETs. Practical applications require that sensors remain stable and operational for at least a month period of time. No prior study of the operation of the aged MoS₂ TF-FETs has been reported. As it will be clear from the further discussion, there are additional reasons why operation of aged TF-FETs is of interest. In addition to the relative change in the source-drain current, $\Delta I_D/I_D$, we used the normalized spectral density of the low-frequency current fluctuations, S_I/I_D^2 , and the

characteristic transient time of the current as the sensing parameters (here, I_D is the source-drain current). Our results show that the aged MoS₂ devices perform better as the sensors in terms of their current stability, sensitivity to the analyte, and reduced contributions of metal contacts to the noise level. Comparison with the graphene FETs reveals significant differences in the effects of exposure to chemical vapors on $\Delta R/R$ and S_I/I_D^2 , suggesting differences in the physical mechanisms of low-frequency current fluctuations.^{17–19}

Thin films of MoS₂ were mechanically exfoliated from bulk crystals and transferred onto Si/SiO₂ substrates following the standard approach.¹ The thickness H of the films ranged from bi-layer to a few layers. Micro-Raman spectroscopy (Renishaw InVia) confirmed the crystallinity and thickness of the MoS₂ flakes after exfoliation. The spectroscopy was performed in the backscattering configuration under $\lambda = 488$ -nm laser excitation using an optical microscope (Leica) with a 50× objective. The excitation laser power was limited to less than 0.5 mW to avoid local heating. Figure 1 shows the schematic of MoS₂ TF-FET (a), optical microscopy image of a representative device (b), and Raman spectrum of the channel material (c). The observed Raman features at ~ 382.9 cm⁻¹ (E_{12g}^1) and ~ 406.0 cm⁻¹ (A_{1g}) are consistent with literature reports.²⁰ Analysis of the Raman spectrum indicates that this sample is 2–3 layer MoS₂ film. The thickness identification is based on the frequency difference, $\Delta\omega$, between the E_{12g}^1 and the A_{1g} peaks. The increase in the number of layers in MoS₂ films is accompanied by the red shift of the E_{12g}^1 and blue shift of the A_{1g} peaks.²⁰

Devices with MoS₂ thin-film channels were fabricated using the electron beam lithography (LEO SUPRA 55) for patterning of the source and drain electrodes and the

^{a)}Author to whom correspondence should be addressed. Electronic mail: balandin@ee.ucr.edu

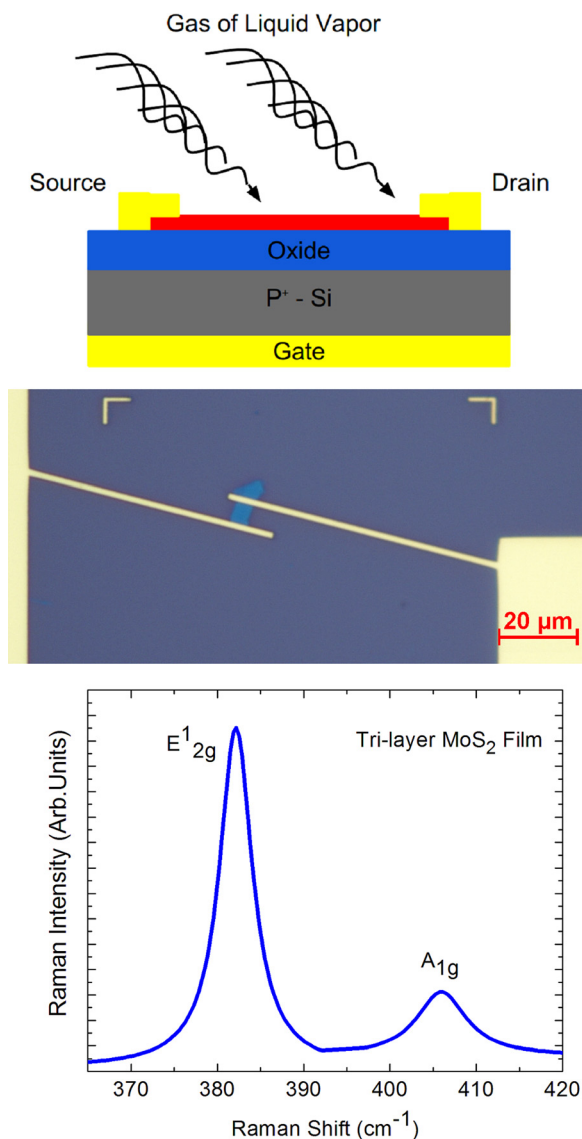


FIG. 1. Schematic of the MoS₂ thin-film sensor with the deposited molecules that create additional charge (upper panel). Optical microscopy image of a representative MoS₂ TF-FET (middle panel). Raman spectrum of the MoS₂ thin-film channel showing the E_{2g}¹ and the A_{1g} peaks. The increase in the number of layers in MoS₂ films is accompanied by the red shift of the E_{2g}¹ and blue shift of the A_{1g} peaks. The energy difference, $\Delta\omega$, between the E_{2g}¹ and the A_{1g} peaks, indicates that the given sample is a tri-layer MoS₂ film.

electron-beam evaporation (Temescal BJD-1800) for metal deposition. The Si/SiO₂ (300-nm) substrates were spin-coated (Headway SCE) and baked consecutively with two positive resists: first, methyl methacrylate (MMA) and then, polymethyl methacrylate (PMMA). The resulting TF-FETs consisted of MoS₂ thin-film channels with Ti/Au (10-nm/100-nm) contacts. The heavily doped Si/SiO₂ wafer served as a back gate. The majority of the bi-layer and tri-layer thickness MoS₂ devices had a channel length, L , in the range from 1.3 μm to 3.5 μm, and the channel width, W , in the range from 1 μm to 6 μm. Some of the devices were covered with 10-nm Al₂O₃ layer to serve as the reference samples in control experiments.

It is known that defective and doped graphene has the greater sensitivity for CO, NO, NO₂, and other gases.²¹ The

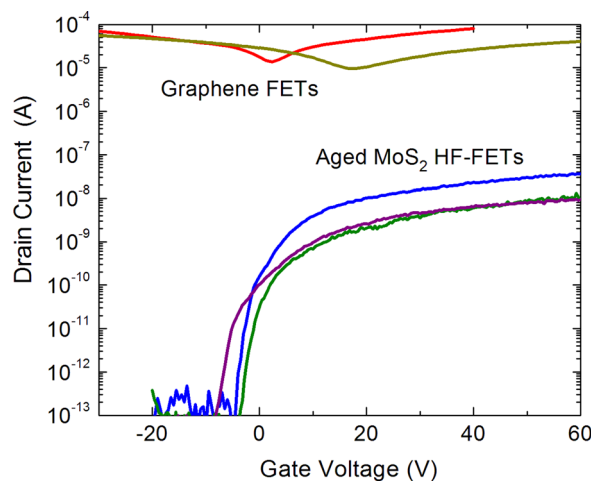


FIG. 2. Current-voltage characteristics of the aged MoS₂ TF-FET used in the study. A typical graphene FET transfer characteristic is also shown for comparison in the same scale. Graphene reveals much higher current owing to superior electron mobility. MoS₂ TF-FET is characterized by better on-off ratio owing to its energy band gap. Different curves correspond to different samples.

same can possibly be true for thin film MoS₂ devices. In particular, it has been shown that the high density of edge states enhances the sensitivity.¹⁶ Therefore, aged, i.e., more defective devices can be more attractive for gas sensing applications. In the present work, we found that aged MoS₂ TF-FETs were more stable and had negligible contact contribution to the drain-to-source resistance. The aged MoS₂ devices were characterized by the on-to-off ratio of $\sim 10^4$, electron mobility $\mu \sim 0.5$ cm²/V s and negligible contact resistance. The new, as fabricated, devices had mobility values in the range from 1 to 8 cm²/V s, which is typical for the back-gated MoS₂ TF-FETs.^{10,22,23} An estimate for the contact resistances was obtained by plotting the drain-to-source resistance, R_{DS} , vs. $1/(V_G - V_{TH})$, and extrapolating this dependence to zero. Figure 2 shows a representative transfer current-voltage (I-V) characteristic for the aged MoS₂ TF-FET used in this study. For comparison, typical I-Vs for a graphene device are also shown. Analyzing I-Vs for MoS₂ thin films and graphene, one can see possible implications for sensor operation: graphene device has much higher currents owing to graphene superb mobility, while MoS₂ devices have better gating and on-off ratio owing to MoS₂ band gap.

For testing the sensor operation, the vapors were produced by bubbling dry air through the respective solvents and diluting the gas flow with the dry air. The resulting concentrations were $\sim 0.5 P/P_0$, where P is the vapor pressure and P_0 is the saturated vapor pressure. When the sample is exposed to the vapor, the vapor molecules, which attach the channel surface, create negative or positive charges at the MoS₂ surface (see Fig. 1(a)). The latter depletes or enhances the electron concentration in the channel depending on the vapor species. For testing MoS₂ TF-FETs, we selected three polar solvents: acetonitrile (CH₃CN—polar aprotic), ethanol (C₂H₅OH—polar protic), and methanol (CH₃OH—polar protic); as well as two non-polar solvents: toluene (C₆H₅-CH₃) and chloroform (CHCl₃).

Figure 3 shows the drain current as a function of time in MoS₂ TF-FET exposed to ethanol, methanol, and acetonitrile,

respectively (from top to bottom). For all chemical vapors, the measurements were conducted at the small drain-source voltage $V_D = 0.1$ V. The high gate bias of $V_G = 60$ V is explained by the presence of 300-nm thick SiO_2 layer in the back gate. One can see from Fig. 3 that in all cases of polar solvents, the drain current increased upon exposure to the vapor and decreased after the vapor exposure was turned off. The results were reproducible for several switching on and off over in a month old MoS_2 TF-FETs tested over a period of few days. The time constants, τ , for I_D increase and decrease were different for each examined analyte. Note that the current of the reference sample—the same device with the channel coated by Al_2O_3 —did not reveal any changes.

Figure 4 presents drain current as a function of time in MoS_2 TF-FET exposed to chloroform and toluene, respectively (from top to bottom). To better illustrate a large range of the current change, Fig. 4 also shows the data for chloroform in a semi-logarithmic scale. The exposure to the vapors of non-polar solvents has an opposite effect on I_D . The drain current reduces by more than two-orders of magnitude, almost completely switching the device off. We found also that the response of the MoS_2 transistors to some vapors demonstrates a memory effect: current remains small or even continue to decrease after the vapor flow is switched off. The current (resistance) is completely restored after gate and voltage biases are set to zero. The τ values were different for each analyte. Although not shown, no changes in current were observed for the reference samples. It is important to note that the data presented in Figs. 3 and 4 were for devices intentionally aged by a month. Initially, the aging study was

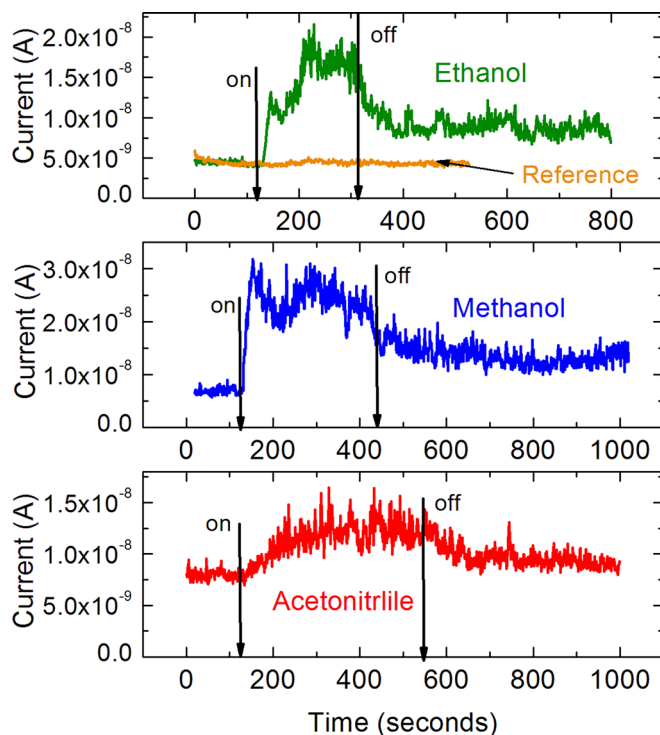


FIG. 3. Drain-source current versus time in MoS_2 TF-FET exposed to the vapors of polar solvents: ethanol (upper panel), methanol (middle panel), and acetonitrile (lower panel). The data were taken at the same gate voltage $V_G = 60$ V and drain voltage $V_D = 0.1$ V for each case. The reference sample—the same device with the Al_2O_3 coated channel—has not revealed any variations in current as shown in the upper panel.

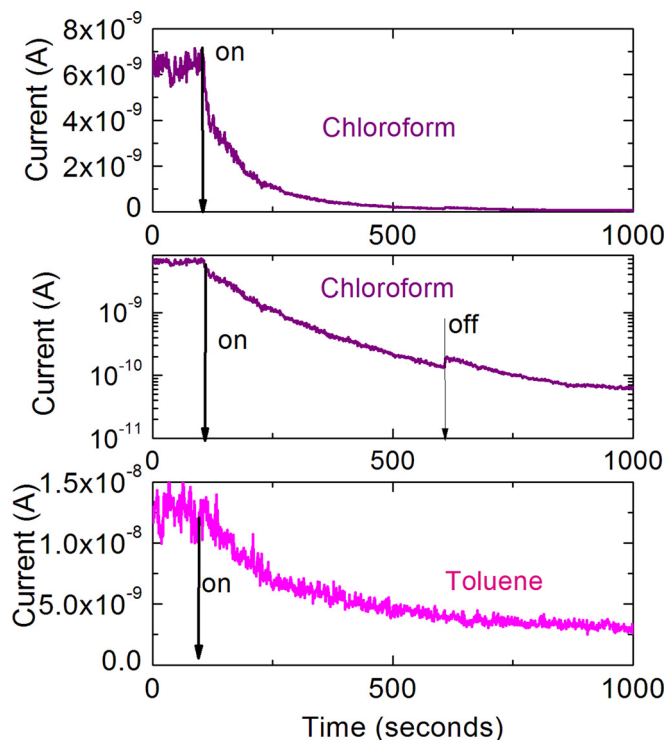


FIG. 4. Drain-source current versus time MoS_2 TF-FET exposed to the vapors of non-polar solvents: chloroform (upper and middle panels) and toluene (lower panel). The data were taken at the same gate voltage $V_G = 60$ V and drain voltage $V_D = 0.1$ V for each case.

performed to verify that MoS_2 TF-FETs maintain their characteristic. Any practical sensor applications require that the FETs are operational for at least a month. Interestingly, we observed that the characteristics of the aged devices even improved in terms of their current stability and sensitivity. The as fabricated MoS_2 TF-FETs responded in the same way to the polar and non-polar analytes as the aged devices.

We have recently demonstrated the use of the low-frequency current fluctuations of I_D in graphene devices as an additional sensing parameter.^{24,25} Some gases induce bulges at characteristic frequencies in the spectral density of the low-frequency current fluctuations S_I/I_D^2 of graphene FETs or change its average value. In order to test the same approach for MoS_2 TF-FETs, we measured the low-frequency noise spectral density in MoS_2 TF-FETs exposed to open air and chemical vapors. The details of our low-frequency measurements have been reported by us elsewhere.²⁶ Figure 5 shows S_I/I_D^2 of MoS_2 TF-FET for different vapors. Red lines show the noise spectra measured in open air with intervals of a few days. The change of the noise spectra was found only as a result of the exposure to the acetonitrile vapor (indicated by green lines). The inset in Fig. 5 magnifies the low-frequency part of spectra indicating good noise spectra measurements reproducibility. One can see that $S_I/I_D^2 \propto 1/f$ (here, f is the frequency) without traces of bulges for all spectra including those measured under acetonitrile vapor. This is in a drastic contrast to graphene devices. In this sense, S_I/I_D^2 is a better sensing parameter for graphene rather than for few-layer MoS_2 films. However, the properly calibrated average level of S_I/I_D^2 can still be used for MoS_2 TF-FETs in combination with τ and $\Delta I_D/I_D$.

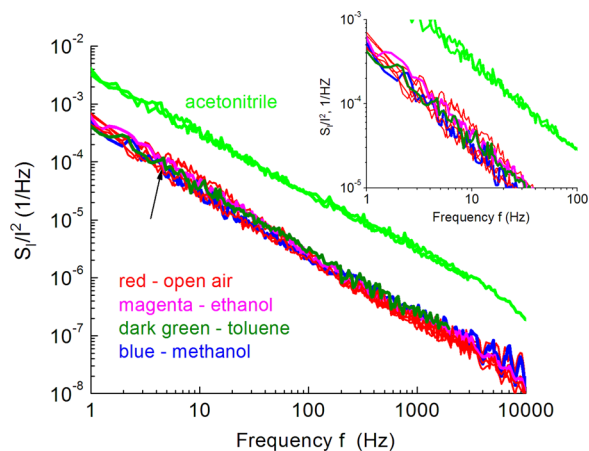


FIG. 5. The normalized spectral density of the low-frequency source-drain current fluctuations measured for MoS₂ TF-FET in open air and under exposure to the vapors. The data were taken at the same gate voltage $V_G = 60$ V and drain voltage $V_D = 0.1$ V for each case. The spectral density of MoS₂ TF-FET under vapor exposure reveals $1/f$ dependence without any traces of bulges unlike graphene FETs. The inset magnifies the low-frequency part of the spectra.

Table I summarizes the data for examined chemical vapors including their type, dielectric constant ϵ , and two sensing parameters. In addition to the relative current change, $\Delta I_D/I_D$, we also show the ratio of the drain current under gas exposure to the initial current before exposure, I_D/I_0 . The I_D/I_0 metric is illustrative for the situation when the drain current decreases. For comparison, the $\Delta I_D/I_D$ data for graphene FETs is also shown. As seen, the presence of the band gap in MoS₂, allows one to achieve a larger change in the current (orders of magnitude in some cases) than in graphene devices. For some vapors, it is possible to completely switch off MoS₂ by the gas. The latter makes MoS₂ very attractive for the gas sensing applications.

Although the exact mechanism of vapor molecule interactions goes beyond the scope of this work and requires atomistic simulations, one can observe certain trends from data in Table I and Figs. 3 and 4. The characteristic time constants for current change under the exposure to polar molecules are much shorter than those for non-polar molecules. The vapors of non-polar solvents, characterized by small ϵ , induce current quenching in the thin MoS₂ channel. The vapors of polar solvents with much larger ϵ , on contrary increase the electrical current in MoS₂ channel likely via inducing additional charges. Indeed, considering that ϵ for a few-layer MoS₂ is around 4,²⁷ the polar molecules would create a much larger dielectric mismatch with MoS₂. There are other possible mechanisms of MoS₂ TF-FET selectivity. It can be related to different binding energies of the gas

molecules attached to the defect sites on MoS₂ film surface. Such a mechanism was proposed to explain selectivity of reduced graphene oxide devices.²⁸ It was proposed that MoS₂ layers tend to interact strongly with the donor-like analytes and their selectivity can be affected by the underlying substrate.¹⁴ Alternatively, there was a suggestion that the exposed edge states in few-layer MoS₂ play the dominant role in selective gas detection.¹⁶ This mechanism assumes that the basal plane, without defects, terminated by S atoms, which lacks dangling bonds, is not active in molecule detection. The edge sites terminated by Mo or S atoms missing coordination bonds are more active in attaching gas molecules.¹⁶ In this scenario, few-layer MoS₂ films with more edge step sites can be preferential at the TF-FET channel.

The absence of bulges in MoS₂ TF-FETs, which is in contrast to graphene FETs, can be related to different mechanisms of low-frequency noise in these two material systems. We have previously shown that low-frequency noise in MoS₂ thin films is similar to that in conventional semiconductors and can be described well by McWhorter model, which assumes that the dominant noise contribution comes from the number of carriers fluctuations.²⁶ Graphene, similar to metals, reveals noise response, which does not comply with the McWhorter model.^{17–19,29,30} Although the low frequency noise mechanism in graphene is still under debates,¹⁹ it is clear now that it is different from that in MoS₂. The latter makes the response of noise to the gas exposure to be also different in these two materials.

In conclusion, we demonstrated selective gas sensing with MoS₂ TF-FETs using the change in the channel current, characteristic transient time, and low-frequency noise spectral density as the sensing parameters. The exposure to ethanol, acetonitrile, toluene, chloroform, and methanol vapors results in drastic changes in the source-drain current. The current can increase or decrease by more than two-orders of magnitude depending on the analyte type (polar vs. non polar). The MoS₂ TF-FETs intentionally aged for a month were robust and demonstrated even better stability and sensitivity. The reference devices with coated channel did not show any response. Unlike graphene devices and thin-film MoS₂ transistors do not show characteristic bulges in the low-frequency current fluctuation spectra. The differences in the low-frequency noise response are likely related to differences in the noise mechanisms and require further study. The tested MoS₂ TF-FETs revealed orders of magnitude change in current (resistance) upon gas exposure, which is in contrast to graphene devices. The obtained results are important for practical applications of MoS₂ thin films and other van der Waals materials.

TABLE I. Chemical vapors and sensing parameters of MoS₂ TF-FET.

Vapor	Type	ϵ	τ (s)	I_D/I_0 MoS ₂ FET	$\Delta I_D/I_D$ (%) MoS ₂ FET	$\Delta I_D/I_D$ (%) graphene FET
Ethanol	Polar protic	24.6	~35	3.778	+300	-50 ^a
Methanol	Polar protic	33.0	~20	3.714	+280	-40 ^a
Acetonitrile	Polar aprotic	37.5	~130	1.625	+60	-35 ^a
Chloroform	Non-polar	4.81	~550	0.231	-75	-25 ^a
Toluene	Non-polar	2.38	~900	0.012	-98	+15 ^a

^aThe data for graphene is taken from Ref. 24.

The work at UC Riverside was supported by the Semiconductor Research Corporation (SRC) and Defense Advanced Research Project Agency (DARPA) through STARnet Center for Function Accelerated nanoMaterial Engineering (FAME). S.L.R. acknowledges partial support from the Russian Fund for Basic Research (RFBR). The work at RPI was supported by the National Science Foundation under the auspices of the EAGER program. Authors thank Dr. V. Tokranov for the help with sample fabrication and Dr. Potyrailo for discussions on gas sensing.

- ¹A. K. Geim and I. V. Grigorieva, *Nature* **499**, 419 (2013).
- ²D. Teweldebrhan, V. Goyal, and A. A. Balandin, *Nano Lett.* **10**, 1209 (2010).
- ³M. Chhowalla, H. S. Shin, G. Eda, L.-J. Li, K. P. Loh, and H. Zhang, *Nat. Chem.* **5**, 263 (2013).
- ⁴Z. Yan, C. Jiang, T. R. Pope, C. F. Tsang, J. L. Stickney, P. Goli, J. Renteria, T. T. Salguero, and A. A. Balandin, *J. Appl. Phys.* **114**, 204301 (2013).
- ⁵J. Heising and M. G. Kanatzidis, *J. Am. Chem. Soc.* **121**, 11720 (1999).
- ⁶Y. Kim, J.-L. Huang, and C. M. Lieber, *Appl. Phys. Lett.* **59**, 3404 (1991).
- ⁷J. L. Verble and T. J. Wieting, *Phys. Rev. Lett.* **25**, 362 (1970).
- ⁸S. W. Han, H. Kwon, S. K. Kim, S. Ryu, W. S. Yun, D. H. Kim, J. H. Hwang, J.-S. Kang, J. Baik, H. J. Shin, and S. C. Hong, *Phys. Rev. B* **84**, 045409 (2011).
- ⁹K. F. Mak, C. Lee, J. Hone, J. Shan, and T. F. Heinz, *Phys. Rev. Lett.* **105**, 136805 (2010).
- ¹⁰G. Eda, H. Yamaguchi, D. Voiry, T. Fujita, M. Chen, and M. Chhowalla, *Nano Lett.* **11**, 5111 (2011).
- ¹¹H. Li, Z. Yin, Q. He, H. Li, X. Huang, G. Lu, D. W. H. Fam, A. I. Y. Tok, Q. Zhang, and H. Zhang, *Small* **8**, 63 (2012).
- ¹²D. J. Late, B. Liu, H. S. S. R. Matte, V. P. Dravid, and C. N. R. Rao, *ACS Nano* **6**, 5635 (2012).
- ¹³Q. He, Z. Zeng, Z. Yin, H. Li, S. Wu, X. Huang, and H. Zhang, *Small* **8**, 2994 (2012).
- ¹⁴F. K. Perkins, A. L. Friedman, E. Cobas, P. M. Campbell, G. G. Jernigan, and B. T. Jonker, *Nano Lett.* **13**, 668 (2013).
- ¹⁵M. Shur, S. Rumyantsev, C. Jiang, R. Samnakay, J. Renteria, and A. A. Balandin, "Selective gas sensing with MoS₂ thin film transistors," in IEEE Sensors 2014, Valencia, Spain, 2–5 November 2014.
- ¹⁶S. L. Zhang, H. H. Choi, H. Y. Yue, and W. C. Yang, *Curr. Appl. Phys.* **14**, 264 (2014).
- ¹⁷M. Z. Hossain, S. Rumyantsev, M. S. Shur, and A. A. Balandin, *Appl. Phys. Lett.* **102**, 153512 (2013).
- ¹⁸S. L. Rumyantsev, D. Coquillat, R. Ribeiro, M. Goiran, W. Knap, M. S. Shur, A. A. Balandin, and M. E. Levinstein, *Appl. Phys. Lett.* **103**, 173114 (2013).
- ¹⁹A. A. Balandin, *Nat. Nanotechnol.* **8**, 549 (2013).
- ²⁰C. Lee, H. Yan, L. E. Brus, T. F. Heinz, J. Hone, and S. Ryu, *ACS Nano* **4**(5), 2695 (2010).
- ²¹K. R. Ratinac, W. Yang, S. P. Ringer, and F. Braet, *Environ. Sci. Technol.* **44**, 1167 (2010).
- ²²H. Wang, L. Yu, Y.-H. Lee, Y. Shi, A. Hsu, M. Chin, L.-J. Li, M. Dubey, J. Kong, and T. Palacios, *Nano Lett.* **12**, 4674 (2012).
- ²³M. Xu, T. Liang, M. Shi, and H. Chen, *Chem. Rev.* **113**, 3766 (2013).
- ²⁴S. Rumyantsev, G. Liu, M. S. Shur, R. A. Potyrailo, and A. A. Balandin, *Nano Lett.* **12**, 2294 (2012).
- ²⁵S. Rumyantsev, G. Liu, R. A. Potyrailo, A. A. Balandin, and M. S. Shur, *IEEE Sens. J.* **13**, 2818 (2013).
- ²⁶J. Renteria, R. Samnakay, S. L. Rumyantsev, C. Jiang, P. Goli, M. S. Shur, and A. A. Balandin, *Appl. Phys. Lett.* **104**, 153104 (2014).
- ²⁷E. J. G. Santos and E. Kaxiras, *ACS Nano* **7**(12), 10741 (2013).
- ²⁸J. T. Robinson, F. K. Perkins, E. S. Snow, Z. Q. Wei, and P. E. Sheehan, *Nano Lett.* **8**, 3137 (2008).
- ²⁹S. Rumyantsev, G. Liu, W. Stillman, M. Shur, and A. A. Balandin, *J. Phys.: Condens. Matter* **22**, 395302 (2010).
- ³⁰G. Liu, S. Rumyantsev, M. S. Shur, and A. A. Balandin, *Appl. Phys. Lett.* **102**, 093111 (2013).